BIOCHEMISTRY
including biophysical chemistry & molecular biology

ARTICLE

pubs.acs.org/biochemistry

Sensitive Detection of Protein−Lipid Interaction Change on Bacteriorhodopsin Using Dodecyl β-D-Maltoside

Takanori Sasaki,*[,†] Makoto Demura,[‡] Noritaka Kato,[†] and Yuri Mukai[†]

[†]School of Science and Technology, Meiji University, Tama-ku, Kawasaki-shi, Kanagawa 214-8571, Japan

[‡]Faculty of Life Science, Hokkaido University, Sapporo 060-0810, Japan

ABSTRACT: A light-driven proton pump bacteriorhodopsin (bR) forms a two-dimensional hexagonal lattice with about 10 archaeal lipids per monomer bR on purple membrane (PM) of *Halobacterium salinarum*. In this study, we found that the weakening of the bR−lipid interaction on PM by addition of alcohol can be detected as the significant increase of protein solubility in a nonionic detergent, dodecyl β-D-maltoside (DDM). The protein solubility in DDM was also increased by bR−lipid interaction change accompanied by structural change of the apoprotein after retinal removal and was about 7 times higher in the case of completely bleached membrane than that of intact PM. Interestingly, the cyclic and milliseconds order of structural change of bR under light irradiation also led to increasing the protein solubility and had a characteristic light intensity dependence with a phase transition. These results indicate that there is a photointermediate in which bR−lipid interaction has been changed by its dynamic structural change. Because partial delipidation of PM by CHAPS gave minor influence for the change of the protein solubility compared to intact PM in both dark and light conditions, it is suggested that specific interactions of bR with some lipids which remain on PM even after delipidation treatment have a key role for the change of solubility in DDM induced by alcohol binding, ligand release, and photon absorption on bR.

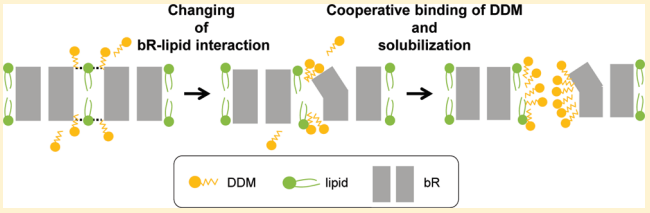

Bacteriorhodopsin (bR) is a light-driven proton pump in the cell membrane of *Halobacterium salinarum*[1] and forms trimers that are arranged as a two-dimensional (2D) hexagonal lattice.[2] bR is closely related to G-protein-coupled receptors, which are main pharmaceutical targets, and widely used as a model for understanding of sensing and signaling by the seven transmembrane helical proteins. On the cell membrane, bR is surrounded by 10 archaeal lipids per monomer[3] and interacts with those lipids by hydrogen bond, salt bridge, and van del Waals contact.[4] bR changes its structure with complete or instantaneous disorder of the 2D lattice mainly at two events: (I) ligand binding/release and (II) formation of photointermediates.[5] In event I, Schiff base binding of the all-*trans*-retinal as a ligand to Lys216 located in the interior of the bacterioopsin (bO) causes a large red shift of the λ_{max} from 380 to 560 nm[6] and subtle tertiary structural change of the protein.[7,8] The 2D lattice of bR called purple membrane (PM), which is very stable up to about 80 °C,[9] is easily destroyed at room temperature when the retinal is released.[8,10] When the retinal is released from bR, the inverse reactions occur. In event II, light-absorbed bR changes its structure dynamically to pump a proton from the cytoplasmic side to the extracellular side on the millisecond time scale.[11,12] So far, the tertiary structures of bR in the ground state[13−16] and some photointermediates[17−24] have been obtained mainly by X-ray and electron crystallography. These structural studies clarified that a large-scale movement of helices E, F, and G on the cytoplasmic side occurs in the late M (M_2, M_N) and N photointermediates:[20,21,25−28] the top end of helix F at the cytoplasmic side and the EF loop are displaced by ∼3.5 and ∼3.0 Å, respectively.[20,21] These movements open a water-accessible channel in the protein, enabling a proton to be taken up from the cytoplasm and the transfer of a proton from D96 to the Schiff base. On this background, some researchers have focused on the change of bR−lipid interaction accompanied by the conformational change of bR. For instance, Bryl and Yoshihara demonstrated that the removal of retinal from bR causes loosening of the lipid packing around the bO by fluorescence measurement in the reconstituted vesicle system.[29] ^{13}C NMR measurement also showed increase in the proportion of surrounding lipids per protein by retinal release.[30] In addition, the elimination of some native lipids from PM affects the photocycle of bR,[31] indicating the importance of the lipid−protein interactions and those dynamic changes for a normal photocycle. However, there is a great lack of convenient techniques to confirm the protein−lipid interaction changes caused by reagents or structural changes of the protein on the native membrane without labeling or chemical modification.

In this study, we report here on the detection of the bR components changed interaction strength with the lipid on PM, by utilizing a nonionic detergent dodecyl β-D-maltoside (DDM) with disaccharide maltose and a C12 of alkyl chain. Although the ground state of bR on PM was resistant to DDM,[32] the solubility of bR in DDM was increased significantly by changing of the bR−lipid interaction after addition of alcohol or retinal removal.

Received: December 15, 2010
Revised: February 7, 2011
Published: February 11, 2011

Calculation of the solubilized protein ratio allowed us to quantify the dissociation constant of the lipid to bR and the protein molecules which have the weakened interaction with lipids by the structural change. Interestingly, the solubility of bR in DDM was also increased by the cyclic and milliseconds order of structural change under light irradiation and showed characteristic light intensity dependence with a phase transition. These results indicate there is the specific photointermediate which has changed the specific protein−lipid interaction compared to that of the ground state. This solubilization technique utilizing the low solubilizing ability of DDM may be applicable as a convenient tool to detect the protein−lipid interaction change irrespective of protein's structural change on the native membrane.

MATERIALS AND METHODS

Sample Preparation. PM of *H. salinarum* strain R1M1 was prepared according to the method of Oesterhelt and Stoeknius.[33] The purified samples were suspended in 5 mM Tris-HCl buffer (pH 7.0). The concentration of PM was determined from absorption maximum at 568 nm using an extinction coefficient of 62700 M^{-1} cm^{-1}.[34] Halorhodopsin from *Natronomonas pharaonis* was prepared as the histidine-tagged protein by expression using *Escherichia coli* BL21 (DE3) cell. Purification procedure of the NpHR was essentially the same as described previously.[43]

The bleached membrane was obtained by illumination of the suspension of 10 μM PM with yellow light in the presence of 300 mM hydroxylamine (Wako, Osaka, Japan). Bleaching ratio was checked by the relative absorbance of the bleached membrane at the peak around 568 nm against to the intact PM. The suspension of bleached membrane was centrifuged with polyallomer centrifuge tube at 46500*g* for 40 min at 4 °C, and the supernatant was removed. The precipitation was washed by repeating three times of dilution by 5 mM Tris-HCl buffer (pH 7.0) and centrifugation to completely remove the hydroxylamine.

Regeneration of bleached membrane to retinal bound membrane was performed by addition of 1 mM (final concentration) all-*trans*-retinal (Sigma-Aldrich Corp., St. Louis, MO, USA) and incubation at 25 °C for 12 h. After regeneration, excess all-*trans*. retinal was removed by centrifugation and washing by 5 mM Tris-HCl buffer.

Delipidated PM was prepared by the method desctribed in ref 32. Briefly, 40 μM PM was incubated in 10 mM MES buffer (pH 5.0) containing 5% (w/v) CHAPS (Dojindo Lab, Kumamoto, Japan) at room temperature for 48 h. Seigneuret et al. report that up to 75% of phospholipids can be removed by incubation with CHAPS.[32] The delipidated PM was washed twice with 5 mM Tris HCl buffer, followed by incubation with 1 mg/nmol PM of Bio-Beads SM-2 Adsorbent (Bio-Rad, Hercules, CA) at room temperature for 2 h. After removal of the Bio-Beads, the delipidated PM was concentrated by centrifugation and stored at 4 °C.

The final concentration of PM and delipidated and bleached membrane used for solubilization experiments was 10 μM, respectively.

Solubilization of PM by Dodecyl β-D-Maltoside. Solubilization experiments of PM and modified membranes were performed with 0.3−30 mM dodecyl β-D-maltoside (DDM) (Dojindo Lab, Kumamoto, Japan) in 5 mM Tris-HCl buffer as a total volume of 1.5 mL. After solibilization treatment at 25 °C for 1−24 h in the dark condition, the sample solution was centrifuged at 142000*g* for 30 min at 4 °C, and the supernatant was regarded as the solubilized bR. The absorption spectra of the solubilized bR and PM were measured by a U-0080D spectrometer (Hitachi, Ibaraki, Japan). The solubilization ratio of the protein was estimated by comparing the absorption maximum of the supernatant at around 280 nm with that of 10 μM bR which was completely solubilized by octyl β-D-glucoside (Dojindo Lab, Kumamoto, Japan), because of minimalization of the light scattering effect.

PM was also solubilized by DDM in the presence of 0.25−0.75 M 1-propanol (Wako, Osaka, Japan). After addition of the designated concentrations of DDM (0−30 mM) and 1-propanol to the 5 mM Tris-HCl buffer, PM was added to the solution. Centrifugation and absorbance determination after solubilization treatment at 25 °C for 24 h were performed as described above.

For solubilization experiment under illumination, the 150 W halogen lamp illuminator equipped with a sharp cut filter Y-52 and a light control was used. Relative light intensities were calculated from the measurement values by a light meter. After incubation at 25 °C for 5−24 h under illumination, the solubilization ratio was estimated as described above.

Circular Dichroism Measurement. Circular dichroic (CD) spectra in the 300−700 nm region were recorded at 25 °C for PM and solubilized bR using a J-820 spectropolarimeter (Jasco, Tokyo, Japan) with a thermostat-controlled cell holder. The path length of the optical cuvette was 10 mm. The speed and number of scans were 200 nm/min and 10 times, respectively.

Gel Filtration Chromatography of the Solubilized bR. Gel filtration chromatography of the DDM-solubilized bR and *N. pharaonis* halorhodopsin (NpHR) was performed by ÄKTA purifier chromatography system (GE Healthcare, Uppsala, Sweden). The DDM−bR complex (10 μM, 250 μL) was applied to a Superdex 200 10/300 GL size exclusion column [total bed volume (V_t) = 24 mL] (GE Healthcare, Uppsala, Sweden) that had been equilibrated previously with 50 mM NaP_i (pH 7.0), 150 mM NaCl, and 0.1% DDM. The column was run at a flow rate of 500 μL/min, and proteins eluted were monitored at 280, 380, and 560 nm, respectively. Standard proteins for calibration of the molecular mass were thyroglobulin (669 kDa), ferritin (440 kDa), aldolase (158 kDa), conalbumin (75 kDa), and ovalbumin (44 kDa). The excluded volumes (V_o) were determined using blue dextran. All samples were chromatographed at 25 °C. Elution of bR and NpHR was detected by the absorbance at 560 and 580 nm, respectively. To prepare a calibration curve of K_{av} values versus log molecular weight, the K_{av} of each protein was calcuated according to the equation:

$$K_{av} = (V_e - V_o)/(V_t - V_o)$$

where V_e is the elution volume for the protein.

RESULTS

Change of bR Solubility in DDM by Addition of Alcohol. At first, we focused on a correlation between the strength of bR−lipid interaction on PM and the solubility of ground state bR in DDM. Alcohol molecules can penetrate primarily within the water/lipid interface, breaking the hydrogen bonds between the lipid headgroup and protein, or the lipid headgroups.[35−39] The alcohol located in the membrane also has a disordering effect on lipid hydrocarbon chains. So we examined the effect of 1-propanol addition to the solubility of intact PM in DDM. Figure 1A and the insertion show UV and CD spectra of 10 μM PM in the absence or presence of 0.25 and 0.5 M 1-propanol, respectively. λ_{max}, maximum absorbance, and the pattern of CD spectra which

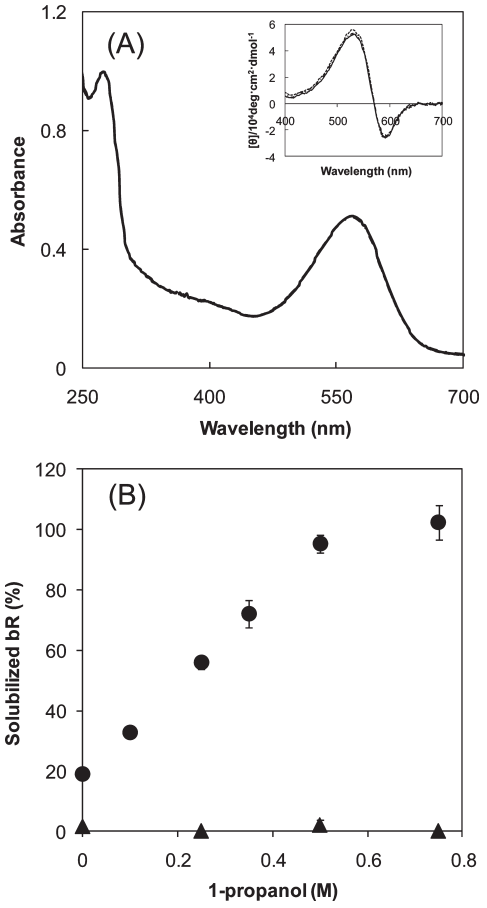

Figure 1. (A) Absorption spectra and CD spectra (insertion) of 10 μM PM in the presence of 0 M (solid line), 0.25 M (dotted line), and 0.5 M (dash-dotted line) 1-propanol. (B) 1-Propanol concentration dependencies for solubilization ratios of bR after incubation in the presence of 20 mM DDM (circles) and absence of DDM (triangles) at 25 °C for 24 h, respectively. Average values ± SD (n = 3).

reflects the trimeric arrangement[40−43] were not changed at all in this 1-propanol concentration range, respectively, indicating that the local retinal environment and quaternary structure of bR on PM have been hardly affected by alcohol. Nevertheless, solubilization ratio of bR in the condition of 20 mM DDM for 24 h at 25 °C was remarkably increased with increasing 1-propanol concentration and reached from 20% to almost 100% by increasing 1-propanol from 0 to 0.5 M (Figure 1B, circles). Solubilized bR by DDM showed an absorption maximum at 551 nm in the dark, blue shifted about 9 nm from that of intact PM (data not shown). These results indicate that breaking of the bR−lipid interaction by the reagent can be detected as increasing the protein solubility in DDM even though the tertiary structure and 2D arrangement of bR have not been changed.

We further investigated DDM concentration dependencies for the solubilization ratio of 10 μM PM in the absence or presence of 0.25 and 0.5 M 1-propanol, respectively. In the absence of 1-propanol, although the percentage of solubilized bR was increased by increasing DDM concentration, that reached plateau of about 20% at around 15−20 mM DDM (Figure 2, circles). These results allow us to define that intact PM is resistant to DDM.[44] Because almost constant solubilization ratios (20−30%) were obtained even when the recovered PM by centrifugation after 20 mM DDM treatment for 24 h was resolubilized, it is

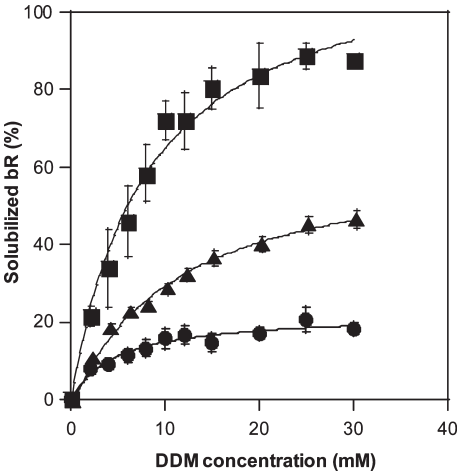

Figure 2. DDM concentration dependencies for solubilization ratios of bR from PM in the presence of 0 M (circles), 0.25 M (triangles), and 0.5 M (squares) 1-propanol after incubation at 25 °C for 24 h, respectively. Average values ± SD (n = 3). Correlation coefficients for the curve fittings were >0.99, respectively.

suggested that solubilized bR and PM exist as a two-state system in the DDM solution, and there is no preferential solubilization by DDM against the different size of membrane or heterogeneous bR component (data not shown). On the other hand, addition of 1-propanol reduced the resistance of PM to DDM and showed strong DDM concentration dependency for the solubilized bR ratio (Figure 2, triangles and squares). Assuming that the solubilized bR is created as a product by the binding and reaction between PM and DDM with specific affinity, these plots were best fitted with the Michaelis−Menten-type equation:

$$A = \frac{A_m[D]}{K_D + [D]} \quad (1)$$

where K_D is the dissociation constant of DDM, [D] is the DDM concentration, A_m is the maximum solubilization ratio, and A is the solubilization ratio. Although A_m values were increased from 22.0% to about 100% with increasing 1-propanol concentration, the K_D values were minor changed to be 4.9, 11.3, and 8.2 mM in the presence of 0, 0.25, and 0.5 M 1-propanol, respectively. These results suggest that the bR−lipid interaction on PM hardly affects the binding step of DDM molecules to the membrane but significantly affects the solubilization step of bR in DDM micelle.

We examined whether solubilized bR by DDM exists as a monomer as previously reported,[32,45] and there is no trimer component. Figure 3 shows the result of gel filtration chromatography of the supernatant (dashed line) and the precipitate (solid line) of bR after DDM solubilization and centrifugation, respectively. The chromatogram of the bR−DDM complex (supernatant) showed a single peak estimated to be 109.4 kDa by the calibration curve with globular protein standards (data not shown). Assuming that bR is solubilized as the monomer, the M_w and number of DDM molecules bound to the bR are calculated to be 82.6 kDa and 161 molecules, respectively (the M_w of one bR and DDM is 26800 and 511, respectively). This calculated number of DDM molecules well corresponds to the reported value of 171 by Møller and le Maire.[46] For comparison, the chromatography for *N. pharaonis* halorhodopsin (NpHR) in a DDM micelle was also performed (dotted line). NpHR is one of the archaeal rhodopsins with about 32000 of the M_w when

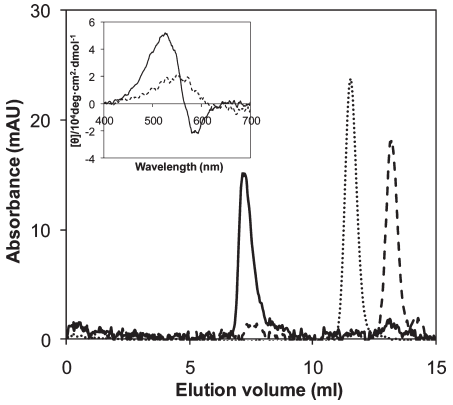

Figure 3. Gel filtration chromatogram of the supernatant (dashed line) and the precipitate (solid line) of bR after solubilization treatment by 20 mM DDM at 25 °C for 144 h and centrifugation. The data of solubilized trimeric NpHR by DDM is also shown (dotted line). Insertion: CD spectra of supernatant (dashed line) and the precipitate (solid line) of bR after solubilization by DDM and centrifugation.

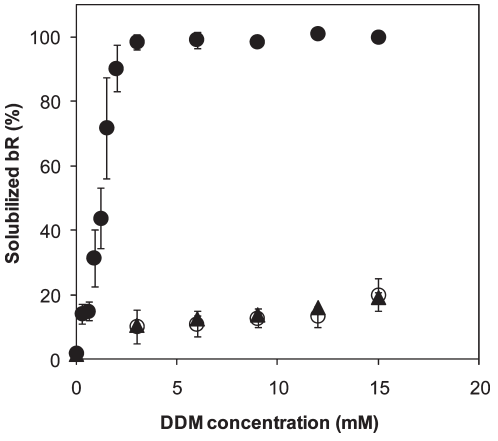

Figure 4. DDM concentration dependencies for solubilization ratios of bR from intact PM (solid triangles), completely bleached PM (solid circles), and regenerated PM (open circles). Each PM (10 μM) was solubilized at 25 °C for 24 h. The data points are the means ± SE of duplicate points from three independent experiments.

including the His tag and known to retain the trimer even in the solubilized state by DDM.[43,47] As a result, the M_w of the trimeric NpHR−DDM complex was estimated to be 235.3 kDa, significantly larger than that of bR−DDM complex. These results indicate that bR has been solubilized as a monomer. The CD spectra of solubilized bR (Figure 3 insertion, dashed line) also showed a broad positive peak characteristic of the monomeric state.[40,41,43] From these results, it is concluded that solubilized bR by DDM exists as a monomer in solution and there is no trimer component.

Solubility of Bleached bR in DDM. To investigate correlation between the tertiary structural change and bR solubility in DDM, we compared the solubilization ratios of intact bR with retinal-released bR. Figure 4 shows DDM concentration dependencies of solubilized proteins from intact PM (solid triangles) and completely photobleached PM [i.e., bacterioopsin (bO)] by hydroxylamine (solid circles). Solubilization ratio of the bleached membrane was increased drastically with increasing DDM concentration at more than the cmc (0.17 mM) and reached almost

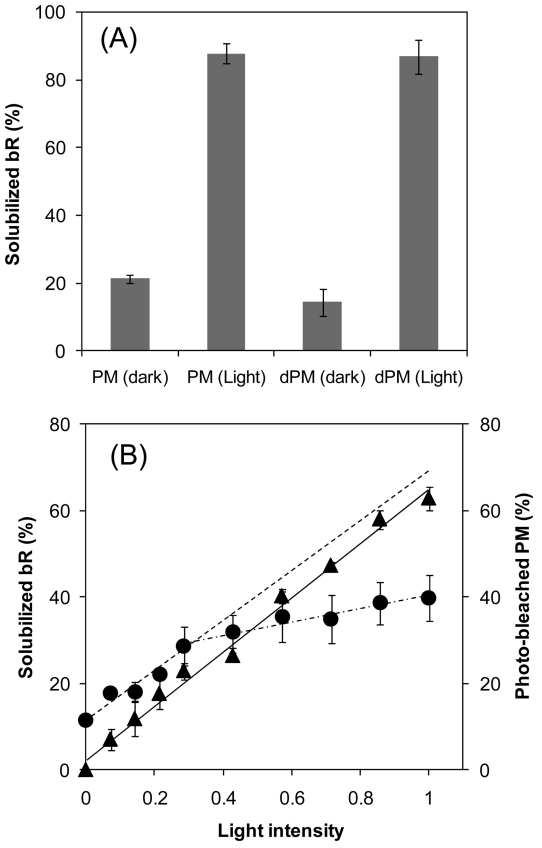

Figure 5. (A) Solubilization ratios of bR by 20 mM DDM from intact PM and delipidated PM (dPM) by CHAPS, respectively. Solubilization treatments were performed in the dark and under illumination (60 W) at 25 °C for 24 h, respectively. Average values ± SD (n = 3). (B) Light intensity dependencies for solubilization ratio of bR by 20 mM DDM after incubation for 5 h at 25 °C (solid circles, assigned to the left axis) and for photobleaching ratio of bR on PM in the presence of 300 mM hydroxylamine after incubation for 1 h at 25 °C (solid triangles, assigned to the right axis). Average values ± SD (n = 3). The values of light intensity were normalized by the maximum intensity of 150 W. Correlation coefficients for the linear fit to the plots of photobleached PM ratio and solubilization ratio were >0.99.

100% in the presence of 3 mM DDM. Contrary to this, regenerated membrane by readdition of sufficient doses of all-*trans*-retinal (open circle) recovered the resistance to DDM: DDM concentration dependency for solubilizaion ratio of regenerated membrane showed almost the same as that of intact PM. These results indicate that the use of DDM enables to detect the bR−lipid interaction change caused by tertiary structural change of the protein.

Solubility of bR under Light Irradiation in DDM. As described in the introduction, it is well-known that light-absorbed bR changes its tertiary structure dynamically to form some photointermediates in photocycle and backs to the ground state in the milliseconds order. To confirm whether formation of the photointermediates changes the strength of the bR−lipid interaction, the solubility of bR in DDM under continuous irradiation with visible light was examined. As a result, the solubilization ratio of bR under light irradiation (60 W) for 24 h was reached about 90%, significantly higher than that in the dark condition (Figure 5A). A large population of the solubilized bR molecules has kept an absorption maximum at around

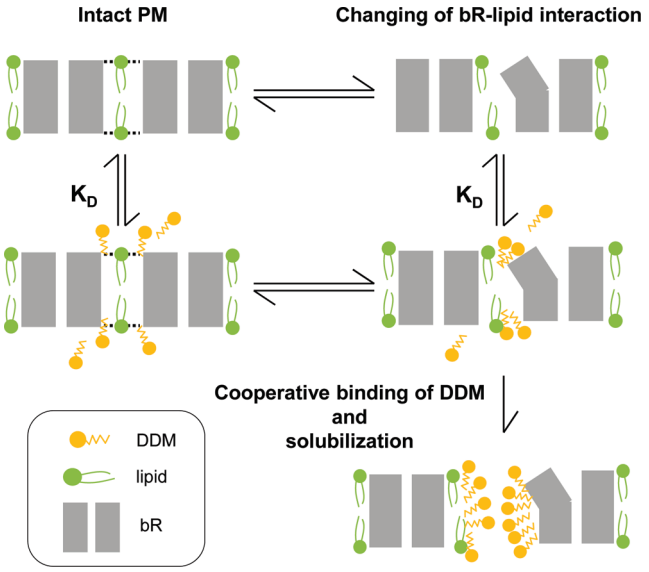

Figure 6. Schematic representation for a correlation between the bR−lipid interaction change accompanied by the reagent addition or the structural change of the prorein and the solubility of bR in DDM. K_L, dissociation constant for the binding of the lipid to bR; K_D, dissociation constant for the binding of DDM to PM.

555 nm (data not shown). This result clearly indicates that there is a photointermediate which weakens the bR−lipid interaction by its dynamic structural change in the millisecond order of photocycle. We further examined DDM solubilization for the partially delipidated PM by CHAPS (Figure 5A). It is previously reported that the total number of bound archaeal lipids per bR is reduced from 10 to 3−4 after 48 h incubation by CHAPS.[32] In both dark and light conditions, the solubilization ratios of bR from this predelipidated PM were almost the same as intact PM. These results indicate that the dynamic structural change of bR can be detected as the change of solubility in DDM, even at the condition that the density of bR molecules on the membrane is increased by delipidation.

Figure 5B (circles) shows the light intensity dependence on the solubilization ratio of bR by 20 mM DDM for 5 h at 25 °C. The solubilization ratio showed the strong light intensity dependence in the low light intensity region of 0−0.3 with the high slope (dotted line). If this slope has been kept even in the high light intensity region, the solubilization ratio at 1.0 of the relative light intensity is predicted to be about 66.2% (the net solubilization ratio of photoactivated bR is about 54.6%). But in fact, the dependence was dramatically reduced in the high light intensity region of 0.3 −1.0 with low slope (dash-dotted line), and observed solubilization at 1.0 of the relative light intensity was only about 39.8% (the net solubilization ratio of photoactivated bR was about 28.2%). It is not likely due to the limitation of the protein solubility by DDM because more than 95% of the protein can be solubilized from the completely bleached membrane by 20 mM DDM treatment for 5 h (data not shown). Next, we measured the light intensity dependence on the photobleaching ratio of bR in the presence of 300 mM hydroxylamine (Figure 5B (triangles)). Interestingly, the photobleaching ratio of bR was increased linearly with increasing light intensity (solid line), showing the different light intensity dependence from that of solubilization ratio. It has been reported that the hydroxylamine can penetrate into the protein preferentially when bR forms L intermediate in photocycle, where bR still does not change the structure dynamically on the cytoplasmic leaflet.[48] These results suggest that the phase transition at around 0.3 of the relative light intensity is ascribed to the limitation of the bR ratio with dynamic structural change at a time (up to about 50% of the photoexcited bR molecules).

DISCUSSION

Correlation between bR Solubility in DDM and bR−Lipid Interaction. Gel filtration chromatography and CD spectra clarified that bR on PM is solubilized to a monomer in DDM (Figure 3), and the solubilized ratio at 25 °C was low even at high DDM concentration (Figure 2). This resistance of PM to DDM is considered to be mainly due to two factors. One is the character of DDM: both headgroup of DDM with disaccharide maltose and moderate length of alkyl chain (C12) probably have less thermodynamic driving force to fractionate or solubilize PM. Another is the strong interaction of bR with some lipid molecules. We demonstrated this factor by solubilization experiment of PM in the presence of low concentration of 1-propanol (Figures 1 and 2).

Are there any specific lipids that contribute to the resistance to DDM? It is known that the hexagonal lattice of PM has been still kept by removal of about half of the normal lipids by ionic detergent with steroid structure: this suggests that remaining lipids after partial delipidation is essential to keep the lattice structure.[45,49] In this study, the change of resistance of PM to DDM by partial delipidation was minor (Figure 5A). These results indicate that specific interaction between bR and some lipids essential to keep the lattice structure contributes to inhibit solubilization of bR by DDM. Related to this, the significant decrease of DDM resistance is reported on 90% delipidated PM after CHAPS/DDM treatment at pH 5.0, 2 M NaCl,[32] supporting the idea that the specific bR−lipid interaction inhibits solubilization of bR by DDM. A little increase of DDM resistance on the partial delipidated PM is probably due to closer interactions between protein−lipid and proteins by reduction of the lattice from 62.4 to 57.3 Å, or 57.9 Å.[49,50] Heyes and El-Sayed also reports that premelting transition of the delipidated PM by CHAPS occurs at significantly higher temperature than that of the native bR (91 °C compared with 80 °C).[51] Although it needs further investigation to identify the lipids essential to the DDM resistance, some lipids that keep strong interaction with protein even after partial delipidation treatment can be considered as candidates. For example, a phosphatidylglycerol (PG) lipid located between helices AB and DE of neighboring bR monomers[15,52] and a sulfated triglycoside lipid (S-TGA-1) in the bR trimer's central pore [53] remain on the membrane even after deoxycholate treatment.[49] It is plausible that one factor for increasing the solubility of bR by 1-propanol addition to PM in this study (Figure 1,2) is due to the breaking of the hydrogen bond, salt bridge, and van del Waals contact between bR and those specific lipids.

Detection of bR−Lipid Interaction Change Accompanied by Structural Change of the Protein. Previously, the deuterium exchange and atomic force microscopy (AFM) experiments showed that removal of the retinal induces subtle changes of the tertiary structure and the loops of bR to the more open conformation.[7,8] Related to this, the change of protein−lipid interaction by retinal removal was observed in the artificial lipid vesicle system.[29] In this study, this protein−lipid interaction change on the membrane was successfully detected as the difference of the solubility between bR and bO in DDM (Figure 4).

Interestingly, the bR solubility was also increased by the cyclic and milliseconds order of structural change after light absorption (Figure 5). Almost the same solubility of the partial delipidated PM as the intact PM under light irradiation (Figure 5A) suggests the existence of a photointermediate that changes interaction between the protein and the specific lipids. Most plausible intermediate in photocycle where solubilization of bR is enhanced is late M (M_2, M_N); this intermediate is formed within 1 ms after illumination and has a lifetime with a few milliseconds per cycle with approximately 10 ms.[54−56] One reason for this is the movement of the lipid arrangement in late M. Electron crystallography has revealed that the movement of helices E, F, and G in the late M and N intermediates appears to cause the movement and disordering of nearby lipids on the cytoplasmic leaflet.[21] Moreover, the PG lipid between the AB and DE helices of neighboring monomers has high flexibility[57] and is predicted to have a functional role in the opening and closing with photointermediate bR.[7] Another reason is the characteristic light intensity dependence on the bR solubilization ratio observed in this study. This light intensity dependence had a phase transition at 0.3 of the relative light intensity (Figure 5B): the reasonable idea to this transition is an appearance of the photointermediate component inhibited the structural change. Experimental support for this idea comes from the electron diffraction data of F219L mutant bR that revealed the M intermediate component before conformational change ascribed to the photocooperativity: the movement of helix F toward neighbors in the hexagonal lattice is so large that it would not allow all molecules to change conformation simultaneously.[21] More recently, by a high-speed atomic force microscopy, it has been observed that the photoactivated bR changes its structure to open form photocooperatively between bRs in the neighboring trimers.[58] These observations lead to the idea that the phase transition on the solubilization ratio in Figure 5B is ascribed to the appearance of the M intermediate before open conformation. As a result, we concluded that the late M formation with open state changes the specific bR−lipid interaction following to the increasing the solubility in DDM.

Detection Mechanism of bR−Lipid Interaction Change by DDM. Finally, a plausible mechanism to explain the change of bR solubility in DDM is shown in Figure 6. Intact bR in the dark has low solubility in DDM because of the strong and specific bR−lipid interactions (Figure 6, left). When these interactions are changed by the addition of reagents such as the alcohol or the structural change of bR, cooperative interaction between DDM molecules bound to the membrane and solubilization of the bR into the DDM micelle proceed (Figure 6, right). In this mechanism, a low solubilizing ability of DDM is useful for sensitive detection of the protein−lipid interaction change and may be also applicable for other membrane proteins to confirm whether those proteins change interaction with lipids by ligand binding/release or environmental change conveniently.

AUTHOR INFORMATION

Corresponding Author

*Phone/fax: +81-44-934-7321. E-mail: tsasaki@isc.meiji.ac.jp.

ACKNOWLEDGMENT

We thank Dr. Shigeki Mitaku (Nagoya University, Japan) for the generous gift of *H. salinarum* strain R1M1.

ABBREVIATIONS

bR, bacteriorhodopsin; bO, bacterioopsin; DDM, dodecyl β-D-maltoside.

REFERENCES

(1) Oesterhelt, D., and Stoekenius, W. (1971) Rhodopsin-like protein from the purple membrane of *Halobacterium halobium*. *Nat. New Biol. 233*, 149–152.

(2) Henderson, R., and Unwin, P. N. T. (1975) Three-dimensional model of purple membrane obtained by electron microscopy. *Nature 257*, 28–32.

(3) Corcelli, A, Lattanzio, V. M., Mascolo, G., Papadia, P., and Fanizzi, F. (2002) Lipid-protein stoichiometries in a crystalline biological membrane: NMR quantitative analysis of the lipid extract of the purple membrane. *J. Lipid Res. 43*, 132–140.

(4) Cartailler, J.-P., and Luecke, H. (2003) X-ray crystallographic analysis of lipid-protein interactions in the bacteriorhodopsin purple membrane. *Annu. Rev. Biophys. Struct. 32*, 285–310.

(5) Saitô, H., Kawase, Y., Kira, A., Yamamoto, K., Tanio, M., Yamaguchi, S., Tuzi, S., and Naito, A. (2007) Surface and dynamic structures of bacteriorhodopsin in a 2D crystal, a distorted or disrupted lattice, as revealed by site-directed solid-state ^{13}C NMR. *Photochem. Photobiol. 83*, 253–262.

(6) Spudich, J. L., McCain, D. A., Nakanishi, K., Okabe, M., Shimizu, N., Rodman, H., Honig, B., and Bogomolni, R. A. (1986) Chromophore/protein interaction in bacterial sensory rhodopsin and bacteriorhodopsin. *Biophys. J. 49*, 479–483.

(7) Cladera, J., Torres, J., and Padrós, E. (1996) Analysis of conformational changes in bacteriorhodopsin upon retinal removal. *Biophys. J. 70*, 2882–2887.

(8) Möller, C., Büldt, G., Dencher, N. A., Engel, A, and Müller, D. J. (2000) Reversible loss of crystallinity on photobleaching purple membrane in the presence of hydroxylamine. *J. Mol. Biol. 301*, 869–879.

(9) Jackson, M. B., and Sturtevant, J. M. (1978) Phase transitions of the purple membranes of *Halobacterium halobium*. *Biochemistry 17*, 911–915.

(10) Braun, T., Backmann, N., Vogtli, M., Bietsch, A., Engel, A., Lang, H.-P., Gerber, C., and Hegner, M. (2006) Conformational change of bacteriorhodopsin quantitatively monitored by microcantilever sensors. *Biophys. J. 90*, 2970–2977.

(11) Lozier, R. H., Bogomolni, R. A., and Stoeckenius, W. (1975) Bacteriorhodopsin: a light-driven proton pump in *Halobacterium Halobium*. *Biophys. J. 15*, 955–962.

(12) Lanyi, J. K. (1993) Proton translocation mechanism and energetics in the light-driven pump bacteriorhodopsin. *Biochim. Biophys. Acta 1183*, 241–261.

(13) Henderson, R., Baldwin, J. M., Ceska, T. A., Zemlin, F., Beckmann, E., and Downing, K. H. (1990) Model for the structure of bacteriorhodopsin based on high-resolution electron cryo-microscopy. *J. Mol. Biol. 213*, 899–929.

(14) Pebay-Peyroula, E., Rummel, G., Rosenbusch, J. P., and Landau, E. M. (1997) X-ray structure of bacteriorhodopsin at 2.5 angstroms from microcrystals grown in lipidic cubic phases. *Science 277*, 1676–1681.

(15) Essen, L. O., Siegert, R., Lehmann, W. D., and Oesterhelt, D. (1998) Lipid patches in membrane protein oligomers: crystal structure of the bacteriorhodopsin-lipid complex. *Proc. Natl. Acad. Sci. U.S.A. 95*, 11673–11678.

(16) Luecke, H., Schobert, B., Richter, H. T., Cartailler, J. P., and Lanyi, J. K. (1999) Structure of bacteriorhodopsin at 1.55 Å resolution. *J. Mol. Biol. 291*, 899–911.

(17) Sass, H. J., Buldt, G., Gessenich, R., Hehn, D., Neff, D., Schlesinger, R., Berendzen, J., and Ormos, P. (2000) Structural alterations for proton translocation in the M state of wild-type bacteriorhodopsin. *Nature 406*, 649–653.

(18) Luecke, H., Schobert, B., Richter, H. T., Cartailler, J. P., and Lanyi, J. K. (1999) Structural changes in bacteriorhodopsin during ion transport at 2 angstrom resolution. *Science 286*, 255–260.

(19) Royant, A., Edman, K., Ursby, T., Pebay-Peyroula, E., Landau, E. M., and Neutze, R. (2000) Helix deformation is coupled to vectorial proton transport in the photocycle of bacteriorhodopsin. *Nature 406*, 645–648.

(20) Subramaniam, S., and Henderson, R. (2000) Molecular mechanism of vectorial proton translocation by bacteriorhodopsin. *Nature 406*, 653–657.

(21) Vonck, J. (2000) Structure of the bacteriorhodopsin mutant F219L N intermediate revealed by electron crystallography. *EMBO J. 19*, 2152–2160.

(22) Takeda, K., Matsui, Y., Kamiya, N., Adachi, S., Okumura, H., and Kouyama, T. (2004) Crystal structure of the M intermediate of bacteriorhodopsin: allosteric structural changes mediated by sliding movement of a transmembrane helix. *J. Mol. Biol. 341*, 1023–1037.

(23) Lanyi, J. K., and Schobert, B. (2007) Structural changes in the L photointermediate of bacteriorhodopsin. *J. Mol. Biol. 365*, 1379–1392.

(24) Yamamoto, M., Hayakawa, N., Murakami, M., and Kouyama, T. (2009) Crystal structures of different substates of bacteriorhodopsin's M intermediate at various pH levels. *J. Mol. Biol. 393*, 559–573.

(25) Dencher, N. A., Dresselhaus, D., Zaccai, G., and Büldt, G. (1989) Structural changes in bacteriorhodopsin during proton translocation revealed by neutron diffraction. *Proc. Natl. Acad. Sci. U.S.A. 86*, 7876–7879.

(26) Nakasako, M., Kataoka, M., Amemiya, Y., and Tokunaga, F. (1991) Crystallographic characterization by X-ray diffraction of the M-intermediate from the photo-cycle of bacteriorhodopsin at room temperature. *FEBS Lett. 292*, 73–75.

(27) Sass, H. J., Schachowa, I. W., Rapp, G., Koch, M. H. J., Oesterhelt, D., Dencher, N. A., and Büldt, G. (1997) The tertiary structural changes in bacteriorhodopsin occur between M states: X-ray diffraction and Fourier transform infrared spectroscopy. *EMBO J. 16*, 1484–1491.

(28) Weik, M., Zaccai, G., Dencher, N. A., Oesterhelt, D., and Hauss, T. (1998) Structure and hydration of the M-state of the bacteriorhodopsin mutant D96N studied by neutron diffraction. *J. Mol. Biol. 275*, 625–634.

(29) Bryl, K., and Yoshihara, K. (2000) The role of chromophore in the lipid-protein interactions in bacteriorhodopsin-phosphatidylcholine vesicles. *FEBS Lett. 480*, 123–126.

(30) Saitô, H., Tsuchida, T., Ogawa, K., Arakawa, T., Yamaguchi, S., and Tuzi, S. (2002) Residue-specific millisecond to microsecond fluctuations in bacteriorhodopsin induced by disrupted or disorganized two-dimensional crystalline lattice, through modified lipid-helix and helix-helix interactions, as revealed by ^{13}C NMR. *Biochim. Biophys. Acta 1565*, 97–106.

(31) Mukhopadhyay, A. K., Dracheva, S., Bose, S., and Hendler, R. W. (1996) Control of the integral membrane proton pump, bacteriorhodopsin, by purple membrane lipids of *Halobacterium halobium*. *Biochemistry 35*, 9245–9252.

(32) Seigneuret, M., Neumann, J. M., and Rigaud, J. L. (1991) Detergent delipidation and solubilization strategies for high-resolution NMR of the membrane protein bacteriorhodopsin. *J. Biol. Chem. 266*, 10066–10069.

(33) Oesterhelt, D., and Stoeckenius, W. (1974) Isolation of the cell membrane of *Halobacterium halobium* and its fractionation into red and purple membrane. *Methods Enzymol. 31*, 667–678.

(34) Rehorek, M., and Heyn, M. P. (1979) Binding of all-*trans*-retinal to the purple membranes. Evidence for cooperativity and determination of the extinction coefficient. *Biochemistry 18*, 4977–4983.

(35) Chin, J. H., and Goldstein, D. B. (1977) Effects of low concentrations of ethanol on fluidity of spin-labeled erythrocyte and brain membranes. *Mol. Pharmacol. 13*, 435–441.

(36) Mitaku, S., Ikuta, K., Itoh, H., Kataoka, R., Naka, M., Yamada, M., and Suwa, M. (1988) Denaturation of bacteriorhodopsin by organic solvents. *Biophys. Chem. 30*, 69–79.

(37) Lu, H. V., and Longo, M. L. (2004) The influence of short-chain alcohols on interfacial tension, mechanical properties, area/molecule, and permeability of fluid lipid bilayers. *Biophys. J. 87*, 1013–1033.

(38) Hayakawa, N., Kasahara, T., Hasegawa, D., Yoshimura, K., Murakami, M, and Kouyama, T. (2008) Effect of xenon binding to a hydrophobic cavity on the proton pumping cycle in bacteriorhodopsin. *J. Mol. Biol. 384*, 812–823.

(39) Gurtovenko, A. A., and Anwar, J. (2009) Interaction of ethanol with biological membranes: the formation of non-bilayer structures within the membrane interior and their significance. *J. Phys. Chem. B 113*, 1983–1992.

(40) Heyn, M. P., Bauer, P.-J., and Dencher, N. A. (1975) A natural CD label to probe the structure of the purple membrane from *Halobacterium halobium* by means of exciton coupling effects. *Biochem. Biophys. Res. Commun. 67*, 897–903.

(41) Hasselbacher, C. A., Spudich, J. L., and Dewey, T. G. (1988) Circular dichroism of halorhodopsin: comparison with bacteriorhodopsin and sensory rhodopsin. *Biochemistry 27*, 2540–2546.

(42) Isenbarger, T. A., and Krebs, M. P. (2001) Thermodynamic stability of the bacteriorhodopsin lattice as measured by lipid dilution. *Biochemistry 40*, 11923–11931.

(43) Sasaki, T., Kubo, M., Kikukawa, T., Kamiya, M., Aizawa, T., Kawano, K., Kamo, N., and Demura, M. (2009) Halorhodopsin from *Natronomonas pharaonis* forms a trimer even in the presence of a detergent, dodecyl-beta-D-maltoside. *Photochem. Photobiol. 85*, 130–136.

(44) Lichtenberg, D., Goñi, F. M., and Heerklotz, H. (2005) Detergent-resistant membranes should not be identified with membrane rafts. *Trends Biochem. Sci. 30*, 430–436.

(45) Tanio, M., Tuzi, S., Yamaguchi, S., Konishi, H., Naito, A., Needleman, R., Lanyi, J. K., and Saitô, H. (1998) Evidence of local conformational fluctuations and changes in bacteriorhodopsin, dependent o lipids, detergents and trimeric structure, as studied by ^{13}C NMR. *Biochim. Biophys. Acta 1375*, 84–92.

(46) Møller, J. V., and le Maire, M. (1993) Detergent binding as a measure of hydrophobic surface area of integral membrane proteins. *J. Biol. Chem. 268*, 18659–18672.

(47) Sasaki, T., Aizawa, T., Kamiya, M., Kikukawa, T., Kawano, K., Kamo, N., and Demura, M. (2009) Effect of chloride binding on the thermal trimer-monomer conversion of halorhodopsin in the solubilized system. *Biochemistry 48*, 12089–12095.

(48) Subramaniam, S., Marti, T., Rösselet, J. S., Rothschild, H. J., and Khorana, H. G. (1991) The reaction of hydroxylamine with bacteriorhodopsin studied with mutants that have altered photocycles: selective reactivity of different photointermediates. *Proc. Natl. Acad. Sci. U.S.A. 88*, 2583–2587.

(49) Grigorieff, N., Beckmann, E., and Zemlin, F. (1995) Lipid location in deoxycholate-treated purple membrane at 2.6 Å. *J. Mol. Biol. 254*, 404–415.

(50) Glaeser, R. M., Jubb, J. S., and Henderson, R. (1985) Structural comparison of native and deoxycholate-treated purple membrane. *Biophys. J. 48*, 775–780.

(51) Heyes, C. D., and El-Sayed, M. A. (2002) The role of the native lipids and lattice structure in bacteriorhodopsin protein conformation and stability as studied by temperature-dependent Fourier transform-infrared spectroscopy. *J. Biol. Chem. 277*, 29437–29443.

(52) Saitô, H., Kawase, Y., Kira, A., Yamamoto, K., Tanio, M., Yamaguchi, S., Tuzi, S., and Naito, A. (2007) Surface and dynamic structures of bacteriorhodopsin in a 2D crystal, a distorted or disrupted lattice, as revealed by site-directed solid-state ^{13}C NMR. *Photochem. Photobiol. 83*, 253–262.

(53) Weik, M., Patzelt, H., Zaccai, G., and Oesterhelt, D. (1998) Localization of glycolipids in membranes by In Vivo labeling and neutron diffraction. *Mol. Cell 1*, 411–419.

(54) Subramaniam, S., Lindahl, M., Bullough, P., Faruqi, A. R., Tittor, J., Oesterhelt, D., Brown, L., Lanyi, J., and Henderson, R. (1999) Protein conformational changes in the bacteriorhodopsin photocycle. *J. Mol. Biol. 287*, 145–161.

(55) Chizhov, I., Chernavskii, D. S., Engelhard, M., Mueller, K. H., Zubov, B. V., and Hess, B. (1996) Spectrally silent transitions in the bacteriorhodopsin photocycle. *Biophys. J. 71*, 2329–2345.

(56) Neutze, R., Pebay-Peyroula, E., Edman, K., Royant, A., Navarro, J., and Landau, E. M. (2002) Bacteriorhodopsin: a high-resolution structural view of vectorial proton transport. *Biochim. Biophys. Acta 1565*, 144–167.

(57) Sato, H., Takeda, K., Tani, K., Hino, T., Okada, T., Nakasako, M., Kamiya, N., and Kouyama, T. (1999) Specific lipid-protein interactions in a novel honeycomb lattice structure of bacteriorhodospin. *Acta Crystallogr. D55*, 1251–1256.

(58) Shibata, M., Yamashita, H., Uchihashi, T., Kandori, H., and Ando, T. (2010) High-speed atomic force microscopy shows dynamic molecular processes in photoactivated bacteriorhodopsin. *Nat. Nanotechnol. 5*, 208–212.

■ NOTE ADDED AFTER ASAP PUBLICATION

After this paper was published online February 28, 2011, a correction was made to equation 1. The revised version was published March 8, 2011.